LEPTOGENESIS ASSISTED BY BUBBLES*

Tomasz P. Dutka

Korea Institute for Advanced Study
85 Hoegi-ro Dongdaemun-gu, Seoul, South Korea

Received 9 December 2025, accepted 24 February 2026, published online 22 April 2026

Leptogenesis is an attractive explanation for the observed baryon asymmetry of our Universe. In these proceedings, we study a framework where thermal leptogenesis occurs during a period of a first-order phase transition (FOPT). Right-handed neutrinos (RHNs) remain massless until bubble nucleation. Their abrupt mass generation leads to rapid decoupling and modifies the usual washout dynamics. Compared to standard thermal leptogenesis, where successful asymmetry requires masses above a certain scale, we find that bubble dynamics can dramatically reduce this scale and also study associated gravitational wave signals observable at terrestrial interferometers.

DOI:10.5506/APhysPolBSupp.19.2-A18

1. Introduction

Within the inflationary paradigm, the present Universe is mostly independent of initial conditions. This forces us to consider a dynamical origin for the observed imbalance between matter and antimatter. Planck data and models of the early Universe's evolution lead to a highly accurate prediction of the ratio [1]

$$Y_B \equiv \left.\frac{n_B - n_{\bar{B}}}{s}\right|_0 = (8.75 \pm 0.23) \times 10^{-11}\,, \tag{1}$$

where n_B and $n_{\bar{B}}$ correspond to the number density of baryons and antibaryons, respectively, s corresponds to the entropy density, and the subscript denotes the present time.

An elegant mechanism to generate the baryon asymmetry dynamically is through the decay of a heavy singlet fermion which carries lepton number, known as thermal leptogenesis [2]. Here, the baryon asymmetry arises from

* Presented at the XLVI International Conference of Theoretical Physics "Matter to the Deepest", Katowice, Poland, 15–19 September, 2025.

a dynamically generated lepton asymmetry via electroweak sphaleron processes, active within $T \in [10^2, 10^{12}]$ GeV. The source of the lepton asymmetry can be elegantly linked to the CP-violating decays of right-handed neutrinos (RHNs) in the type-I seesaw mechanism [3–7]. The out-of-equilibrium condition, necessary for successful baryogenesis, can be naturally provided by the expansion of the Universe; as the temperature drops below the mass of the lightest RHN, the RHN decays remain efficient, whereas the inverse process becomes Boltzmann-suppressed.

As a consequence of the high-energy scales required, testing the minimal (hierarchical) model is challenging to say the least. On the other hand, if $B-L$ is promoted to a good symmetry which is broken spontaneously and this transition is first-order, in principle, we may be able to indirectly test for leptogenesis by searching for gravitational wave signals produced during bubble percolation. However, most of the parameter space (strong-washout leptogenesis) remains outside the sensitivity range of future gravitational wave detectors as the peak frequency is expected to be high, $f_{\rm peak} \sim 10^5$–10^6 Hz $(T_*/10^{11}$ GeV$)$, where T_* is the reheating temperature of the phase transition. Without modifications, one of which we explore in this work, the prospects for testability are bleak.

We consider bubble dynamics during a first-order phase transition as a source of a strong departure from thermal equilibrium on the RHN population [8]. We show that, in this scenario, the required value of M_N is more than one order of magnitude lower than that of the conventional scenario when requiring successful leptogenesis, and therefore it is within the testable range of future gravitational wave detectors.

2. Setup

The setup of the scenario we consider is as follows: we assume that the Majorana masses of the RHNs are provided by the v.e.v. of a scalar field and the phase transition corresponding to this spontaneous symmetry breaking is first-order. The relevant part of the Lagrangian can be written in the mass basis of the RHNs as

$$\mathcal{L}_{\rm int} = \frac{1}{2}\sum_I y_I \Phi \bar{N}_I^c N_I + \sum_{\alpha,I} Y_{{\rm D},\alpha I} H \bar{L}_\alpha N_I + {\rm h.c.}\,, \tag{2}$$

where L_α are the SM lepton doublets, N_I are the three families of heavy right-handed neutrinos, $Y_{{\rm D},\alpha I}$ are the *Dirac* Yukawa couplings between N_I and L_α, and y_I are *Majorana* Yukawa couplings. After the phase transition,

$\langle \Phi \rangle \equiv v_\phi/\sqrt{2}$, and the type-I seesaw Lagrangian is recovered with $M_I = \frac{1}{\sqrt{2}} y_I v_\phi$. As we assume that the critical temperature of the Φ phase transition is much greater than that of the electroweak critical temperature, we assume $\langle H \rangle = 0$ during and after the FOPT but fix $\langle H \rangle \neq 0$ where appropriate.

With these assumptions, the typical temperature evolution of the conventional thermal leptogenesis scenario can be modified in the following way: RHNs are massless (ignoring thermal effects) until the phase transition of Φ after which they suddenly become massive within the bubbles of the broken phase. As soon as $M_I \neq 0$, the RHNs decay and generate a nonzero lepton asymmetry very rapidly, owing to the strong-washout regime typically predicted in the type-I seesaw. If the bubble nucleation temperature $T_{\rm nuc}$ is significantly smaller than the masses of the RHNs, the inverse decays within the bubbles will be immediately Boltzmann-suppressed and, in principle, $\kappa_{\rm wash} \sim \mathcal{O}(1)$. This is summarised in the left plot of figure 1.

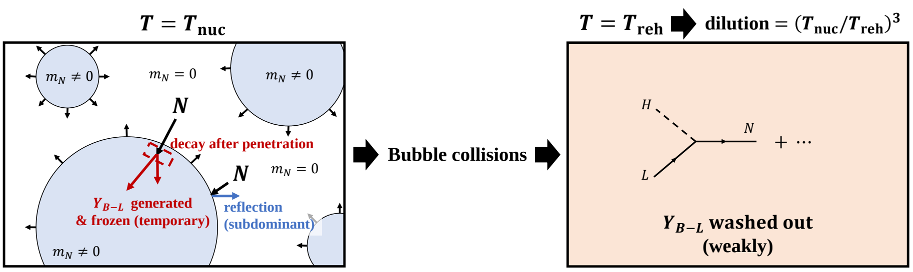

Fig. 1. Schematic picture of the bubble-assisted leptogenesis scenario during bubble expansion (left) and after bubble collisions (right). Figure taken from [8].

The scenario introduces new dynamics which can severely affect this simple qualitative picture and must be properly estimated. During the bubble expansion, the latent heat stored in the scalar potential ΔV, which is the difference in the scalar potential energy density between the true and the false vacuum, is converted to a combination of bubble wall kinetic energy and fluid bulk motion. After the bubble walls and fluid shells collide, this latent heat reheats the background plasma, increasing the temperature to $T_{\rm reh} \sim (\Delta V + \rho_{\rm plasma}(T_{\rm nuc}))^{1/4}$.

The reheating affects our scenario in two ways: *(i)* as the asymmetry is generated during the bubble expansions, it will be diluted by a factor of $(T_{\rm nuc}/T_{\rm reh})^3$ due to reheating, *(ii)* in order to avoid a strong washout, we also require $M_N/T_{\rm reh} \gg 1$ along with $M_N/T_{\rm nuc} \gg 1$, otherwise the RHN inverse decays become rapid after the bubbles collide. This is represented by the right plot of figure 1.

2.1. Cosmological First Order Phase Transitions Basics

For a given tree-level Lagrangian of Φ, the effective potential acquires quantum corrections at zero temperature. The one-loop contribution from a particle i can be written as [9]

$$V_{\rm CW}\left(m_i^2(\phi)\right) = (-1)^{2s_i} g_i \frac{m_i^4(\phi)}{64\pi^2}\left[\log\left(\frac{m_i^2(\phi)}{\mu^2}\right) - c_i\right], \tag{3}$$

where ϕ is the real part of Φ, $\phi \equiv \sqrt{2}\,{\rm Re}(\Phi)$, $m_i(\phi)$ and s_i are the ϕ-dependent mass and spin of a particle i with g_i degrees of freedom. Here, μ is the renormalization scale, and c_i is a constant depending on the subtraction scheme; for the $\overline{\rm MS}$ scheme, $c_i = 3/2$ for $s_i \in \{0, 1/2\}$ and $c_i = 5/6$ for $s_i = 1$.

At a finite temperature T, thermal effects can be captured by including the *thermal potential* of the form

$$V_T\left(m_i^2(\phi)\right) = \pm\frac{g_i}{2\pi^2}T^4 J_{\rm B,F}\left(\frac{m_i^2(\phi)}{T^2}\right) \tag{4}$$

with

$$J_{\rm B,F}\left(y^2\right) = \int\limits_0^\infty {\rm d}x\; x^2 \log\left[1 \mp \exp\left(-\sqrt{x^2+y^2}\right)\right], \tag{5}$$

where the upper (lower) sign is for the bosonic (fermionic) case. In our numerical calculations we use the full form for $J_{\rm B,F}$. For illustrative purposes, we show the expansions of $J_{\rm B}(y^2)$ [10]:

$$\begin{aligned} J_{\rm B}\left(y^2 \ll 1\right) &\approx -\frac{\pi^2}{45} + \frac{\pi^2}{12}y^2 - \frac{\pi}{6}y^3 + \cdots, \\ J_{\rm B}\left(y^2 \gg 1\right) &\approx -\sum_{n=1}^{20}\frac{1}{n^2}y^2 K_2(y\cdot n), \end{aligned} \tag{6}$$

where $K_2(z)$ is the Bessel function of the second-kind. Note that bosonic interactions are required to make the phase transition first order due to the y^3 term in $J_{\rm B}(y^2 \ll 1)$.

Once the temperature-dependent scalar potential is calculated, we obtain the bounce solution and the bounce action using Mathematica based on the well-known overshoot/undershoot method. Additionally, we crosscheck our results against CosmoTransition [11] and FindBounce [12].

The bubble nucleation rate can be estimated as the probability to have a critical bubble per unit time and unit volume, where the origin of this configuration can be either due to quantum or thermal fluctuations. We approximate it as

$$\Gamma(T) \sim \max\left[T^4\left(\frac{S_3}{2\pi T}\right)^{3/2}\exp(-S_3/T),\quad R_0^{-4}\left(\frac{S_4}{2\pi}\right)^2\exp(-S_4)\right], \quad (7)$$

where S_3 and S_4 are $O(3)$ (thermal) and $O(4)$ (quantum) bounce actions, respectively, and R_0 is the initial bubble radius. Since the bubble-assisted leptogenesis framework requires the FOPT not to be too strongly supercooled, the $O(3)$ bounce solution always dominates so we ignore contributions from S_4.

At the critical temperature $T = T_{\rm crit}$, the two local minima are degenerate, and $\Gamma(T_{\rm crit}) = 0$. Thus, in any first-order phase transition, there is a period where $\Gamma(T)$ is much slower than the Hubble expansion rate. During this period, although bubbles can be nucleated, the expansion of spacetime is more efficient and the phase transition does not proceed. The Universe is supercooled until $\Gamma(T)$ becomes comparable to the Hubble rate, $H(T)^4$.

When $\Gamma(T) \sim H(T)^4$, the average distance of two nearby bubble nucleations becomes less than the horizon size and the bubble expansion can physically reduce the volume of the false vacuum. We define this temperature as $T_{\rm nuc}$, $\Gamma(T_{\rm nuc}) \equiv H(T_{\rm nuc})^4$, which can be approximately calculated by solving

$$\frac{S_3(T_{\rm nuc})}{T_{\rm nuc}} \approx 4\log\left[\frac{T_{\rm nuc}}{H(T_{\rm nuc})}\right], \quad (8)$$

where $H(T_{\rm nuc})$ should include the contribution of the vacuum energy that comes from the scalar potential.

The strength of an FOPT is parameterized by

$$\alpha_n \equiv \frac{\Delta V}{\rho(T_{\rm nuc})}, \quad (9)$$

where $\rho(T) = \frac{\pi^2}{30} g_* T^4$ is the plasma energy density which has g_* effective relativistic degree of freedom at T. Since ΔV will eventually be converted to plasma energy after bubble collisions, we can obtain the reheating temperature by

$$\rho(T_{\rm reh}) \simeq \rho(T_{\rm nuc}) + \Delta V, \quad (10)$$

where we assumed that the time scale of the reheating procedure is much shorter than the Hubble time scale. Since $\rho \propto T^4$, the dilution factor after bubble collisions is simply given by

$$\left(\frac{T_{\rm nuc}}{T_{\rm reh}}\right)^3 \simeq (1+\alpha_n)^{-3/4}. \quad (11)$$

3. Leptogenesis inside bubbles

How efficiently the massless RHNs outside of the expanding bubbles can penetrate the bubble wall is an important ingredient, as their penetration causes a large departure from the equilibrium number density of (the now massive) RHNs within the bubbles. An order-one penetration rate, $\kappa_{\rm pen}$, is desired for bubble-assisted leptogenesis.

The penetration rate is closely related to the bubble wall velocity. The fraction of heavy particles entering the wall will grow with the boost factor of the wall, $\gamma_{\rm w}$, and reach an order of one fraction when $M_N \lesssim \gamma_{\rm w} T_{\rm nuc}$. The pressure also increases with the boost factor, requiring a stronger release of energy ΔV, and thus favoring a larger α_n. The details of the penetration rate calculations are found in [8] and figure 2 demonstrates that for sufficiently fast bubble walls, this penetration rate can be almost maximal.

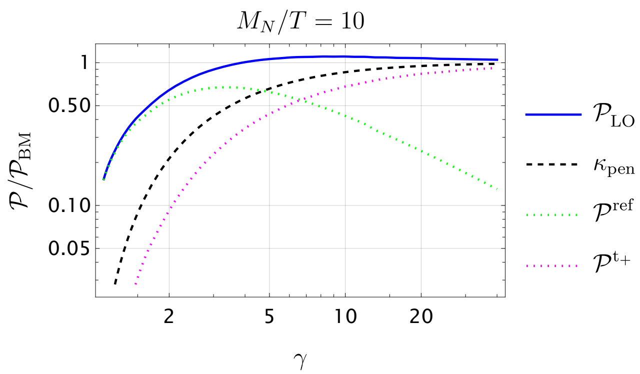

Fig. 2. Penetration rate of RHNs as a function of the bubble wall speed. Figure taken from [8].

Utilising $\kappa_{\rm pen}$, we solve the Boltzmann equations to evolve the initial, non-thermal number densities of N which penetrate the bubble, and calculate the generated lepton asymmetry. In what follows, we will assume that the heavy neutrinos N are in kinetic equilibrium with the SM thermal bath *also inside the bubble*, thanks to the efficient rate for $\phi N \to \phi N$ via N mediation. This will permit us to use integrated Boltzmann equations. The Boltzmann equation in this procedure can be written as

$$\begin{aligned} \dot{n}_{N_I} + 3Hn_{N_I} &= -\sum_{A,B} \left(2\langle\sigma v\rangle_{N_I N_I \to AB}\, n_{N_I}^2 - 2\langle\sigma v\rangle_{AB \to N_I N_I}\, n_A n_B\right) \\ &\quad - \mathit{\Gamma}_D(N_I) n_{N_I}\,, \qquad (12) \\ \dot{n}_{B-L} + 3Hn_{B-L} &= -\sum_I \epsilon_I \mathit{\Gamma}_D(N_I) n_{N_I} + (\text{wash-out})\,. \qquad (13) \end{aligned}$$

Here, n_X denotes the number density of the species X, H is the Hubble expansion rate, and $\dot{n}$ represents a derivative with respect to cosmic time. The quantity $\langle \sigma v \rangle$ denotes the thermally averaged cross section times relative velocity. Furthermore, $\Gamma_D(N_I)$ is the total decay rate of N_I and ϵ_I is the corresponding CP-violating parameter.

There are various reactions relevant to the above Boltzmann equations. At a minimum, the reaction rate of processes involving ϕ must be sizable since we need $y \sim \mathcal{O}(1)$ to ensure that $M_N/T_{\rm nuc} \sim y\, v_\phi/\sqrt{2}\, T_{\rm nuc}$ is large enough to achieve wash-out suppression. Additionally, one must make sure to take into account *unavoidable* depletion processes such as $NN \to \phi\phi$ $N_I N_I \leftrightarrow N_J N_J$ which serve as processes which reduce the number density of RHNs available to decay in a asymmetry generating way. These are especially important as the masses of the RHNs are taken to be smaller [8].

The end of the phase transition occurs once the bubbles have collided, which results in a temperature increase from $T_{\rm nuc} \to T_{\rm reh}$. We quantify the effect of bubble collisions by solving the above Boltzmann equations a second time, with new initial conditions for Y_N and Y_{B-L}

$$Y_N\left(z_{\rm reh}\right) = \tilde{Y}_N \left(\frac{T_{\rm nuc}}{T_{\rm reh}}\right)^3 , \quad Y_{B-L}\left(z_{\rm reh}\right) = \tilde{Y}_{B-L} \left(\frac{T_{\rm nuc}}{T_{\rm reh}}\right)^3 , \quad z_{\rm reh} = \frac{M_N}{T_{\rm reh}} , \tag{14}$$

for $z \in [z_{\rm reh}, z_{\rm f}]$. We choose $z_{\rm f} \gg 1$ such that the final asymmetry no longer changes for larger z, where $\tilde{Y}_N$ and $\tilde{Y}_{B-L}$ were obtained from the previous step. Then, the final baryon abundance is taken as

$$Y_B = \kappa_{\rm sph}\, Y_{B-L}\left(z_{\rm f}\right) , \tag{15}$$

where $\kappa_{\rm sph} = 28/79$ is the usual weak sphaleron conversion factor.

3.1. Results

Figure 3 shows a summary of our results. Here, the grey bands show the amount of enhancement we obtain compared to the conventional thermal leptogenesis, and the horizontal axis shows the strength of the supercooling, α_n. We obtain an $\mathcal{O}(20)$ enhancement compared to conventional scenarios for $M_N = 5 \times 10^9$ GeV.

Combining the enhancement/suppression of RHN decay during and after the expansion of the bubble wall, the final baryon asymmetry in the bubble-assisted leptogenesis mechanism can be expressed in a familiar way as

$$Y_B = Y_N^{\rm eq} \epsilon_{\rm CP}\, \kappa_{\rm sph}\, \kappa_{\rm pen}\, \kappa_{\rm dep}\, \kappa_{\rm wash} \left(\frac{T_{\rm nuc}}{T_{\rm reh}}\right)^3 , \tag{16}$$

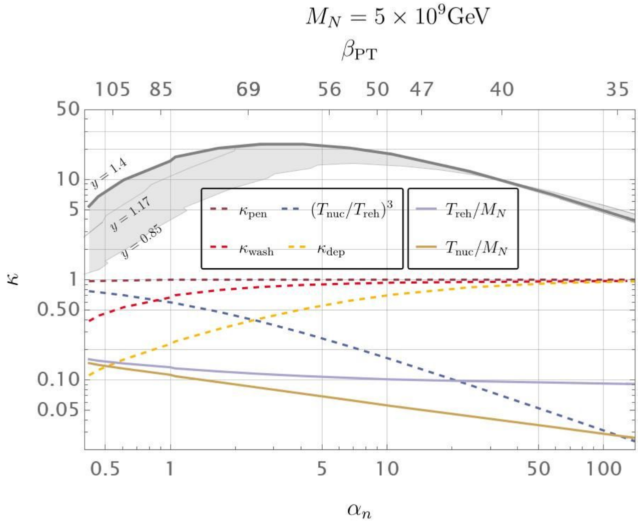

Fig. 3. Presentation of the enhancement in baryon asymmetry generated as a function of the phase transition strength $\propto \alpha_n$. The enhancement of Y_B in the bubble-assisted leptogenesis scenario compared to the conventional thermal leptogenesis scenario is depicted by the grey band.

where $Y_N^{\rm eq}$ is population of RHNs outside the bubbles. For our numerical calculation, we solve the full Boltzmann equations from which each factor can be inferred. Each suppression channel, which we label κ_i, is also shown on the lower part of the plot. The parameters, $\kappa_{\rm pen}$, $\kappa_{\rm wash}$, $\kappa_{\rm dep}$, and $(T_{\rm nuc}/T_{\rm reh})^3$ are shown by the dark red, bright red, yellow, and blue dashed curves, respectively. The penetration coefficient, $\kappa_{\rm pen}$, remains close to unity in our chosen parameter space but begins to decrease for $\alpha_n \lesssim 1$ (reducing the overall asymmetry). Smaller values of α_n imply a large washout, $\kappa_{\rm wash}$ and $\kappa_{\rm dep}$, as the ratio $M_N/T_{\rm reh}$ decreases. Much larger values of α_n however, suffer from a large diluting effect: $(T_{\rm nuc}/T_{\rm reh})^3 = (1+\alpha_n)^{-3/4}$, also reducing the final asymmetry. The enhancement is maximized around $\alpha_n \sim 5$, since Y_B is proportional to the combination of all these factors.

3.2. Gravitational waves

We also investigate the possibility of testing this scenario via gravitational wave detectors, as the collisions of the bubbles required by this scenario necessarily generate gravitational waves. As we find that bubble-assisted leptogenesis is viable for low values of M_N (and therefore low values of the symmetry-breaking scale), the peak frequency of gravitational waves produced can be within the observable range of terrestrial observers such as

ET [13], CE [14], and LIGO O5 [15] as demonstrated in figure 4. Larger values of M_N, which are still viable in the bubble-assisted leptogenesis scenario, would require detectors that can probe higher frequency ranges with existing proposals, *e.g.* Refs. [16–18], albeit with improved sensitivities.

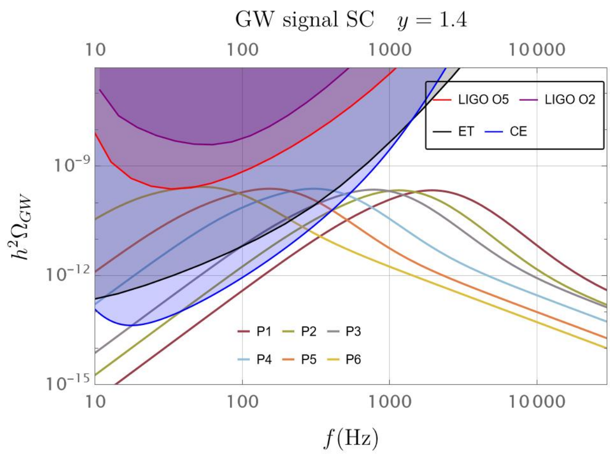

Fig. 4. GW signal from leptogenesis for various benchmark points summarized in [8].

4. Conclusion

We have analyzed how a first-order phase transition can enhance thermal leptogenesis when right-handed neutrinos acquire their masses during the transition. Although the resulting departure from equilibrium suppresses the usual wash-out effects, additional dilution mechanisms, such as reheating and CP-conserving $2 \to 2$ depletions limit the overall gain, and a systematic method to account for all such contributions is provided in [8]. The enhancement is largest for $M_N \sim 10^9$–10^{10} GeV, where an $\mathcal{O}(10$–$10^2)$ increase in the baryon asymmetry relative to the standard scenario is possible. The associated first-order transition also generates gravitational waves with peak frequencies $\mathcal{O}(10^2$–$10^4)$ Hz, and models with $M_N \lesssim 5 \times 10^9$ GeV fall within the projected reach of upcoming detectors such as ET, CE, and LIGO O5, making this parameter region experimentally testable.

The author would like to thank Eung Jin Chun, Tae Hyun Jung, Xander Nagels, and Miguel Vanvlasselaer for their collaboration on the projects mentioned in these proceedings. T.P.D. is supported by KIAS Individual Grants under grant No. PG084101 at the Korea Institute for Advanced Study.

REFERENCES

[1] Planck Collaboration (P.A.R. Ade *et al.*), *Astron. Astrophys.* **594**, A13 (2016).

[2] M. Fukugita, T. Yanagida, *Phys. Lett. B* **174**, 45 (1986).

[3] P. Minkowski, *Phys. Lett. B* **67**, 421 (1977).

[4] T. Yanagida, *Prog. Theor. Phys.* **64**, 1103 (1980).

[5] R.N. Mohapatra, G. Senjanovic, *Phys. Rev. Lett.* **44**, 912 (1980).

[6] S.L. Glashow, *NATO Sci. Ser. B* **61**, 687 (1980).

[7] M. Gell-Mann, P. Ramond, R. Slansky, *Conf. Proc. C* **790927**, 315 (1979).

[8] E.J. Chun *et al.*, *J. High Energy Phys.* **2023**, 164 (2023).

[9] S. Coleman, E. Weinberg, *Phys. Rev. D* **7**, 1888 (1973).

[10] D. Curtin, P. Meade, H. Ramani, *Eur. Phys. J. C* **78**, 787 (2018).

[11] C.L. Wainwright, *Comput. Phys. Commun.* **183**, 2006 (2012).

[12] V. Guada, M. Nemevšek, M. Pintar, *Comput. Phys. Commun.* **256**, 107480 (2020).

[13] M. Maggiore *et al.*, *J. Cosmol. Astropart. Phys.* **03**, 050 (2020).

[14] M. Evans *et al.*, `arXiv:2109.09882 [astro-ph.IM]`.

[15] LIGO Scientific Collaboration (B.P. Abbott *et al.*), *Rep. Prog. Phys.* **72**, 076901 (2009).

[16] V. Domcke, C. Garcia-Cely, N.L. Rodd, *Phys. Rev. Lett.* **129**, 041101 (2022).

[17] A. Berlin *et al.*, *Phys. Rev. D* **105**, 116011 (2022).

[18] A. Berlin *et al.*, *Phys. Rev. D* **108**, 084058 (2023), `arXiv:2303.01518 [hep-ph]`.